

Self-Oscillation in Spin Torque Oscillator Stabilized by Field-like Torque

Tomohiro Taniguchi, Sumito Tsunegi, Hitoshi Kubota, and Hiroshi Imamura
*National Institute of Advanced Industrial Science and Technology (AIST),
 Spintronics Research Center, Tsukuba 305-8568, Japan*
 (Dated: August 19, 2018)

The effect of the field-like torque on the self-oscillation of the magnetization in spin torque oscillator with a perpendicularly magnetized free layer was studied theoretically. A stable self-oscillation at zero field is excited for negative β while the magnetization dynamics stops for $\beta = 0$ or $\beta > 0$, where β is the ratio between the spin torque and the field-like torque. The reason why only the negative β induces the self-oscillation was explained from the view point of the energy balance between the spin torque and the damping. The oscillation power and frequency for various β were also studied by numerical simulation.

Self-oscillation of the magnetization in a nanomagnet excited by spin torque has attracted much attention for its potential application to spintronics devices such as microwave generators, magnetic sensors, and a recording and reading head of high-density hard disk drives [1–7]. Recent development on the enhancement of the perpendicular magnetic anisotropy of the CoFeB ferromagnetic layer by adding a MgO capping layer [8–10] enables us to realize a spin torque oscillator (STO) with a perpendicularly magnetized free layer and an in-plane magnetized pinned layer. It was previously shown that this type of STO produced a high emission power ($\sim 0.5 \mu\text{W}$) with a narrow linewidth ($\sim 50 \text{ MHz}$) by this self-oscillation [11]. It should be noted that in Ref. [11], a relatively large magnetic field (from 2 to 3 kOe) was applied to STO normal to the film plane, while the self-oscillation at zero field was interesting from a practical point of view. Although the emission power at zero field was investigated experimentally, the observed value was very low (typically, a few nW) [12].

Unfortunately, it was theoretically shown that the self-oscillation could not be excited in this type of STO in the absence of the applied field [13]. Above the critical current at which the spin torque destabilizes the perpendicularly magnetized initial state, the magnetization directly moves to the anti-parallel direction with respect to the pinned layer magnetization, and stops its dynamics. This conclusion was analytically shown by calculating the energy balance between the work done by spin torque and the energy dissipation due to the damping, and was confirmed by the numerical simulation of the Landau-Lifshitz-Gilbert (LLG) equation [13].

The purpose of this letter is to show that the previous conclusion is drastically modified by taking into account the field-like torque because the presence of such torque modifies the energy balance between the spin torque and the damping. The numerical simulation of the LLG equation shows that a stable self-oscillation can be realized for a negative β , where β is the ratio between the spin torque and the field-like torque, as defined in Eq. (1) below. We also calculate the current dependences of the power and the oscillation frequency of STO at a finite temperature. The power significantly increases above the critical current when $\beta < 0$, whereas it rapidly decreases when $\beta = 0$

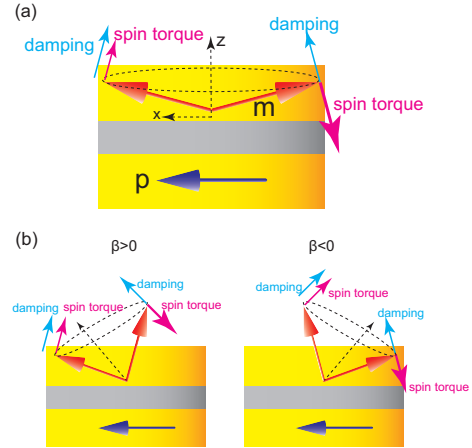


FIG. 1: (a) Schematic view of the system. The unit vectors pointing in the magnetization directions of the free and the pinned layers are denoted as \mathbf{m} and \mathbf{p} , respectively. The directions of the spin torque and the damping are indicated by the red and blue arrows, respectively. The spin torque strength near the anti-parallel alignment of \mathbf{m} and \mathbf{p} is larger than that near the parallel alignment for $\lambda > 0$, where λ is defined in Eq. (2). (b) Schematic view of the magnetization dynamics in the presence of the field-like torque with $\beta > 0$ or $\beta < 0$.

or $\beta > 0$. Also, the oscillation frequency remains relatively high for $\beta < 0$, whereas it drops to approximately zero for $\beta = 0$ and $\beta > 0$.

Figure 1 (a) schematically shows the system under consideration. The unit vectors pointing in the magnetization directions of the free and pinned layers are denoted as \mathbf{m} and \mathbf{p} , respectively. The z -axis is normal to the film plane whereas the x -axis is parallel to the pinned layer magnetization. The current flowing along the z -axis is denoted as I , where the positive current $I > 0$ corresponds to the electrons flowing from the free layer to the pinned layer. As long as the current flows uniformly along the z -axis and the magnetization dynamics is well described by the macrospin model, the following result is applicable to both the nano-pillar and nano-contact. The pinned layer magnetization \mathbf{p} is assumed to be fixed. The magnetization dynamics of the free layer are described by

the LLG equation [14–18],

$$\begin{aligned} \frac{d\mathbf{m}}{dt} = & -\gamma\mathbf{m} \times \mathbf{H} - \gamma H_s \mathbf{m} \times (\mathbf{p} \times \mathbf{m}) \\ & - \gamma\beta H_s \mathbf{m} \times \mathbf{p} + \alpha \mathbf{m} \times \frac{d\mathbf{m}}{dt}, \end{aligned} \quad (1)$$

where γ and α are the gyromagnetic ratio and the Gilbert damping constant, respectively. Throughout this letter, we consider the case of the zero applied field. The magnetic field $\mathbf{H} = (H_K - 4\pi M)m_z\mathbf{e}_z$ consists of the crystalline anisotropy field H_K and the demagnetization field $4\pi M$. Because we are interested in the perpendicularly magnetized free layer, H_K should be larger than $4\pi M$. The magnetic field can be defined as the derivative of the energy density $E = -M(H_K - 4\pi M)m_z^2/2$ with respect to the magnetization $M\mathbf{m}$, i.e., $\mathbf{H} = -\partial E/\partial(M\mathbf{m})$. The effect of the Oersted field generated by the current, which causes a non-uniform magnetization dynamics and whose order is less than or equal to 10 Oe for the experimental parameters [11], is neglected because the experimental results on the oscillation properties of this type of STO was quantitatively reproduced by the macrospin model [11]. The second and third terms on the right-hand side of Eq. (1) represent the spin torque and the field-like torque, respectively. The spin torque strength,

$$H_s = \frac{\hbar\eta I}{2e(1 + \lambda\mathbf{m} \cdot \mathbf{p})MV}, \quad (2)$$

consists of the volume of the free layer V and the spin torque parameters, η and λ . The parameter η corresponds to the spin polarization of the injected current, i.e., the spin polarization of the pinned layer, and λ determines the dependence of the spin torque strength on the relative angle between the magnetizations, \mathbf{m} and \mathbf{p} . The theoretical relation between λ and the material parameters depend on the model [16–19]. For example, Ref. [19] calculated the spin torque from the transfer matrix of a magnetic tunnel junction (MTJ), and showed that $\lambda = \eta\eta'$, where η' is the spin polarization of the free layer. The sign of λ is positive (negative) when the MTJ shows the positive (negative) tunnel magnetoresistance. For the positive (negative) λ , the spin torque magnitude near the anti-parallel alignment of \mathbf{m} and \mathbf{p} is larger (smaller) than that near the parallel alignment [17]. The self-oscillation can be realized when the energy supplied by the spin torque balances with the energy dissipation due to the damping. The energy supplied by the spin torque can be both positive and negative, depending on the current direction and the sign of λ . The net energy supplied during a precession should be positive to excite a stable self-oscillation. In the present geometry with the positive current $I > 0$, the spin torque dissipates energy when $m_x > 0$ because it is parallel to the damping, whereas it supplies energy when $m_x < 0$ because it is anti-parallel to the damping, as shown in Fig. 1 (a). Then, the sign of λ should be positive to make the net energy supplied by the spin torque positive.

On the other hand, the net energy supplied by the spin torque becomes positive by the negative current when λ is negative. Then, only the positive (negative) current can excite the self-oscillation of the magnetization for the positive (negative) λ [2, 13].

The dimensionless parameter β in Eq. (1) is the ratio between the spin torque and the field-like torque. The origin of the field-like torque is the same as that of the spin torque, i.e., the transfer of the transverse spin angular momentum from the conduction electron to the free layer magnetization. While the magnitude of the field-like torque is negligible in a giant magnetoresistive (GMR) system [20, 21], in an MTJ it reaches a few tens of percents of the spin torque magnitude [22, 23]. The value of β has been experimentally measured by using the spin torque diode effect [24–26], although the spin torque diode effect can measure β below the critical current only while the self-oscillation state is realized by the current above the critical current. Another method to estimate β is the measurement of the magnetization switching probability in the thermally activated region [27, 28], in which the effect of the field-like torque is regarded as an enhancement or a reduction of the switching barrier height, and the magnitude of β is estimated from the bias dependence of the switching probability. Both the theoretical calculation and the experimental measurement have shown that the magnitude and sign of the field-like torque depend on the material parameters such as the exchange splitting of the conduction electrons of the free and pinned layers, the sample thickness, and the bias voltage [20–26]. However, for simplicity, β in this letter is assumed to be constant with respect to the bias voltage (current). Instead, we study the magnetization dynamics for various values of β . The value of $|\beta|$ estimated from the spin torque diode measurement of the in-plane magnetized CoFeB/MgO/CoFeB MTJ [25, 26] is on the order of 0.01 – 0.1. Similar values of β were found from the measurement of the switching probability [27, 28].

Figures 2 (a), (b), and (c) show the time evolutions of the components of \mathbf{m} obtained by numerically solving Eq. (1), in which the values of β are (a) $\beta = 0$, (b) 0.2, and (c) -0.2 , respectively. The schematic views of the magnetization dynamics are also shown on the right side. The values of the parameters are $M = 1448$ emu/c.c., $H_K = 20.0$ kOe, $V = \pi \times 60 \times 60 \times 2$ nm³, $\eta = 0.54$, $\lambda = \eta^2$, $I = 1.5$ mA, $\gamma = 1.732 \times 10^7$ rad/(Oe·s), and $\alpha = 0.005$, respectively [8, 10, 11, 29]. By using these parameters, the critical current to destabilize the initial state for $\beta = 0$, $I_c = [4aeMV/(\hbar\eta\lambda)](H_K - 4\pi M)$ [13], is estimated to be 1.2 mA, which corresponds to 11×10^6 A/cm² in terms of the current density. As studied in Ref. [13], in the absence of the field-like torque ($\beta = 0$), the magnetization moves to the anti-parallel direction with respect to $\mathbf{p} = \mathbf{e}_x$, and stops its dynamics. Similarly, in the case of the positive β , the magnetization stops at $\mathbf{m} = -\mathbf{p}$. The convergence time of the magnetization for $\beta > 0$ is shorter than that for $\beta = 0$. Contrary to $\beta \geq 0$, stable self-oscillation is realized for negative β , as shown

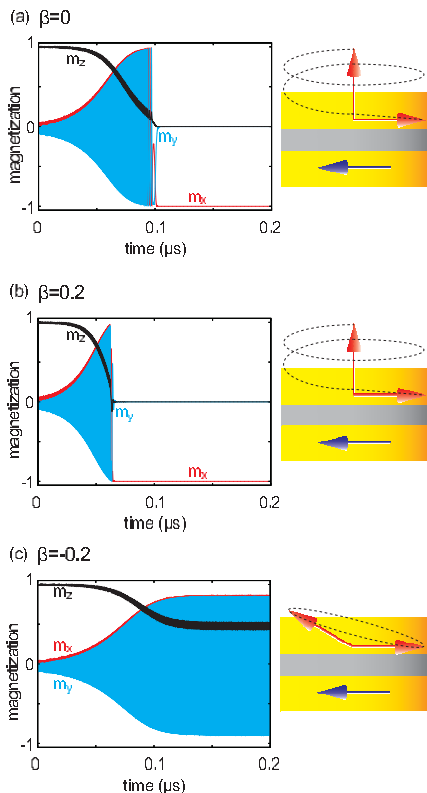


FIG. 2: The time evolutions of the components of \mathbf{m} for (a) $\beta = 0$, (b) 0.2, and (c) -0.2 , where the red, blue, and black lines correspond to m_x , m_y , and m_z , respectively. The current magnitude is 1.5 mA. The magnetization stops at $\mathbf{m} = -\mathbf{p}$ for $\beta = 0$ and 0.2, while it steadily precesses for $\beta = -0.2$. The schematic views of the magnetization dynamics are shown on the right side.

in Fig. 2 (c). The cone angle at the self-oscillation state increases as the current increases.

The results shown in Fig. 2 indicate that the field-like torque plays a key role toward the realization of self-oscillation in this STO. As mentioned after Eq. (2), the self-oscillation can be realized when the energy supplied by the spin torque balances with the energy dissipation due to the damping. For $\beta = 0$, in the absence of the applied field, spin torque above I_c always overcomes the damping during $m_z = 1$ to $m_z = 0$, whereby self-oscillation cannot be realized [13]. The magnetization moves to the film-plane and stops its dynamics at $\mathbf{m} = -\mathbf{p}$. In the case of $\beta \neq 0$, the field-like torque acts approximately as an applied field pointing in the positive (negative) x -direction for $\beta > 0$ (< 0), and modifies the precession trajectory, as shown in Fig. 1 (b), due to which the amount of energy supplied by the spin torque differs from that for $\beta = 0$ [30]. For the positive β , the amount of energy supplied by the spin torque increases, and the magnetization rapidly moves to $\mathbf{m} = -\mathbf{p}$, as shown in Fig. 2 (b). On the other hand, for the negative β , the energy supplied decreases. Then, the spin torque balances with the damping above the film-plane, and therefore, the stable self-oscillation of the magnetization can be realized. In Fig. 3, the oscillation trajectories

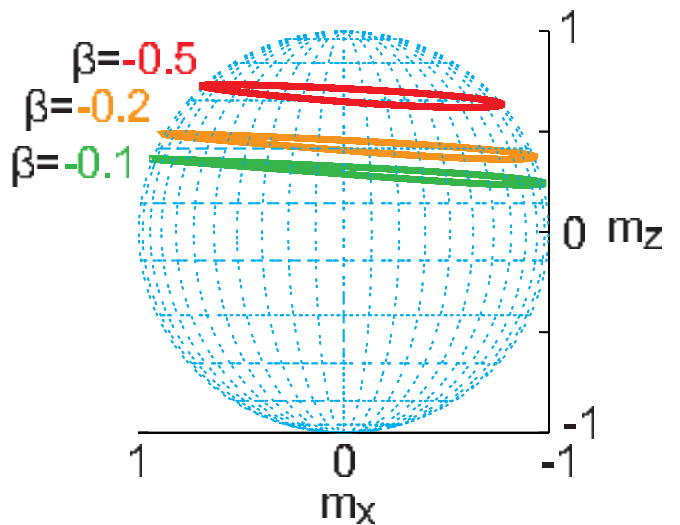


FIG. 3: Trajectories of the steady state precession of the magnetization in the free layer for various negative $\beta = -0.1, -0.2, -0.5$. The current magnitude is $I = 2.0$ mA.

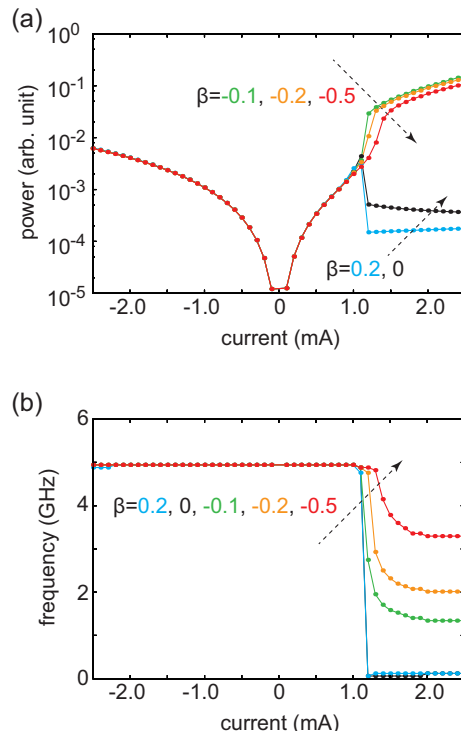


FIG. 4: Dependences of (a) the powers and (b) the oscillation frequencies of STO on the applied current obtained from finite temperature simulations, where the value of β varies from -0.5 to 0.2. The current 1.0 mA corresponds to 8.8×10^6 A/cm².

of the magnetization in the steady state for various negative $\beta = -0.1, -0.2, -0.5$ are shown, where the cone angle of the magnetization from the z -axis increases as the absolute value of β decreases. This is because the amount of the energy supplied by the spin torque increases as $|\beta|$ decreases. It can also be seen from Fig. 3 that the oscillation trajectories are not centered around the z axis.

We also calculated the power and oscillation frequency

of STO, both of which depend on $m_x(t)$ through the magnetoresistance effect $\propto \Delta R \mathbf{m} \cdot \mathbf{p}$ [11], where $\Delta R = R_{\text{AP}} - R_{\text{P}}$ is the difference in the resistances between the parallel (P) and anti-parallel (AP) alignments of \mathbf{m} and \mathbf{p} . The power is defined as $\int_0^\infty |m_x(f)|^2 df$ [11], where $m_x(f)$ is the Fourier transformation of $m_x(t)$. The random torque, $-\gamma \mathbf{m} \times \mathbf{h}$, is added to the right-hand side of Eq. (1). This random torque excite a small amplitude oscillation of the magnetization, known as the mag-noise. Then, even if $\beta \geq 0$, the spectrum has a peak at the ferromagnetic resonance frequency, and the power can be evaluated, although a sustainable oscillation cannot be excited at zero temperature. The components of the random field h_k ($k = x, y, z$) satisfy the fluctuation-dissipation theorem [31], $\langle h_k(t) h_\ell(t') \rangle = [2\alpha k_B T / (\gamma M V)] \delta_{k\ell} \delta(t - t')$, where T is the temperature. The oscillation frequency is defined as the peak frequency of $|m_x(f)|$. The values of the parameters are those used in Fig. 2 with $T = 300$ K. Because of the presence of the random torque, the trajectories of the magnetization dynamics include randomness. Therefore, we repeated the numerical simulation 10^3 times with different random numbers, and averaged these spectra to calculate the power and oscillation frequency.

Figures 4 (a) and (b) show the powers and oscillation frequencies for various β , respectively. Only the positive current can induce the magnetization dynamics in this system [13], and the power observed in the negative current region corresponds to the mag-noise power. We focus on the positive current region here. The most remarkable point is that the power significantly increases above the critical current ($\simeq 1.2$ mA) for $\beta < 0$, whereas it decreases for $\beta = 0$ and $\beta > 0$. This is because, as shown in Fig. 2, the stable self-oscillation of the magnetization can be realized in the case of $\beta < 0$ whereas the magnetization dynamics stop at $\mathbf{m} = -\mathbf{p}$ in the cases of $\beta = 0$ and $\beta > 0$. As shown in Fig. 3, the cone angle of the magnetization from the z -axis increases as the absolute value of β decreases for negative β . Since the large amplitude of m_x due to the large cone angle re-

sults the large power, the power for $\beta = -0.1$ is greater than that for $\beta = -0.5$. On the other hand, the oscillation frequency ($\simeq \gamma(H_K - 4\pi M)m_z / (2\pi)$) decreases as the cone angle of the magnetization, $\cos^{-1} m_z$, increases. Then, the oscillation frequency for $\beta = -0.1$ is lower than that for $\beta = -0.5$. In the cases of $\beta = 0$ and $\beta > 0$, the powers are the mag-noise powers originated from the random oscillation of the magnetization around the z - or x -axis, depending on whether the current magnitude is below or above the critical current. Because the oscillation amplitude of m_x for the precession around the z -axis is larger than that for the precession around the x -axis, the power drops at the critical current. The oscillation frequency above the critical current is almost zero because the anisotropy field $(H_K - 4\pi M)m_z$ is zero in the xy -plane.

In conclusion, the magnetization dynamics of STO with a perpendicularly magnetized free layer and an in-plane magnetized pinned layer was studied by numerically solving the LLG equation. We found that the field-like torque with negative β enabled the realization of a stable large amplitude self-oscillation of the magnetization at zero field in this type of STO, where β is the ratio between the spin torque and the field-like torque. On the other hand, the large amplitude oscillation at zero field cannot be excited for $\beta = 0$ and $\beta > 0$. From the thermally activated state below the critical current to the self-oscillation state slightly above the critical current, the power increases 10^3 times for $\beta < 0$, where the power is defined as the product of the integral of the Fourier spectrum of the oscillation amplitude and the square of the current. The oscillation frequency defined as the peak frequency of the Fourier spectrum remains on the order of a few GHz for $\beta < 0$ as the current increases.

The authors would like to acknowledge H. Maehara, A. Emura, T. Yorozu, S. Tamaru, H. Arai, M. Konoto, K. Yakushiji, T. Nozaki, A. Fukushima, K. Ando, and S. Yuasa. This work was supported by JSPS KAKENHI Number 23226001.

-
- [1] S. I. Kiselev, J. C. Sankey, I. N. Krivorotov, N. C. Emley, R. J. Schoelkopf, R. A. Buhrman, and D. C. Ralph, *Nature* **425**, 380 (2003).
 - [2] W. H. Rippard, M. R. Pufall, S. Kaka, S. E. Russek, and T. J. Silva, *Phys. Rev. Lett.* **92**, 027201 (2004).
 - [3] D. Houssameddine, U. Ebels, B. Delaët, B. Rodmacq, I. Firastrau, F. Ponthenier, M. Brunet, C. Thirion, J.-P. Michel, L. Prejbeanu-Buda, et al., *Nat. Mater.* **6**, 447 (2007).
 - [4] S. Bonetti, P. Muduli, F. Mancoff, and J. Akerman, *Appl. Phys. Lett.* **94**, 102507 (2009).
 - [5] K. Kudo, T. Nagasawa, K. Mizushima, H. Suto, and R. Sato, *Appl. Phys. Express* **3**, 043002 (2010).
 - [6] H. Suto, T. Nagasawa, K. Kudo, K. Mizushima, and R. Sato, *Appl. Phys. Express* **4**, 013003 (2011).
 - [7] J. Sinha, M. Hayashi, Y. K. Takahashi, T. Taniguchi, M. Drapeko, S. Mitani, and K. Hono, *Appl. Phys. Lett.* **99**, 162508 (2011).
 - [8] S. Yakata, H. Kubota, Y. Suzuki, K. Yakushiji, A. Fukushima, S. Yuasa, and K. Ando, *J. Appl. Phys.* **105**, 07D131 (2009).
 - [9] S. Ikeda, K. Miura, H. Yamamoto, K. Mizunuma, H. D. Gan, M. Endo, S. Kanai, J. Hayakawa, F. Matsukura, and H. Ohno, *Nat. Mater.* **9**, 721 (2010).
 - [10] H. Kubota, S. Ishibashi, T. Saruya, T. Nozaki, A. Fukushima, K. Yakushiji, K. Ando, Y. Suzuki, and S. Yuasa, *J. Appl. Phys.* **111**, 07C723 (2012).
 - [11] H. Kubota, K. Yakushiji, A. Fukushima, S. Tamaru, M. Konoto, T. Nozaki, S. Ishibashi, T. Saruya, S. Yuasa, T. Taniguchi, et al., *Appl. Phys. Express* **6**, 103003 (2013).
 - [12] Z. Zeng, G. Finocchio, B. Zhang, P. K. Amiri, J. A. Ka-

- tine, I. N. Krivorotov, Y. Huai, J. Langer, B. Azzerboni, K. L. Wang, et al., *Sci. Rep.* **3**, 1426 (2013).
- [13] T. Taniguchi, H. Arai, S. Tsunegi, S. Tamaru, H. Kubota, and H. Imamura, *Appl. Phys. Express* **6**, 123003 (2013).
- [14] E. M. Lifshitz and L. P. Pitaevskii, *Statistical Physics (part 2), course of theoretical physics volume 9* (Butterworth-Heinemann, Oxford, 1980), chap. 7, 1st ed.
- [15] T. L. Gilbert, *IEEE Trans. Magn.* **40**, 3443 (2004).
- [16] J. C. Slonczewski, *Phys. Rev. B* **39**, 6995 (1989).
- [17] J. C. Slonczewski, *J. Magn. Magn. Mater.* **159**, L1 (1996).
- [18] J. C. Slonczewski, *J. Magn. Magn. Mater.* **247**, 324 (2002).
- [19] J. C. Slonczewski, *Phys. Rev. B* **71**, 024411 (2005).
- [20] S. Zhang, P. M. Levy, and A. Fert, *Phys. Rev. Lett.* **88**, 236601 (2002).
- [21] M. Zwierzycki, Y. Tserkovnyak, P. J. Kelly, A. Brataas, and G. E. W. Bauer, *Phys. Rev. B* **71**, 064420 (2005).
- [22] I. Theodonis, N. Kioussis, A. Kalitsov, M. Chshiev, and W. H. Butler, *Phys. Rev. Lett.* **97**, 237205 (2006).
- [23] J. Xiao and G. E. W. Bauer, *Phys. Rev. B* **77**, 224419 (2008).
- [24] A. A. Tulapurkar, Y. Suzuki, A. Fukushima, H. Kubota, H. Maehara, K. Tsunekawa, D. D. Djayaprawira, N. Watanabe, and S. Yuasa, *Nature* **438**, 339 (2005).
- [25] H. Kubota, A. Fukushima, K. Yakushiji, T. Nagahama, S. Yuasa, K. Ando, H. Maehara, Y. Nagamine, K. Tsunekawa, D. D. Djayaprawira, et al., *Nat. Phys.* **4**, 37 (2008).
- [26] J. C. Sankey, Y.-T. Cui, J. Z. Sun, J. C. Slonczewski, R. A. Buhrman, and D. C. Ralph, *Nat. Phys.* **4**, 67 (2008).
- [27] Z. Li, S. Zhang, Z. Diao, Y. Ding, X. Tang, D. M. Apalkov, Z. Yang, K. Kawabata, and Y. Huai, *Phys. Rev. Lett.* **100**, 246602 (2008).
- [28] W. Rippard, R. Heindl, M. Pufall, S. Russek, and A. Kos, *Phys. Rev. B* **84**, 064439 (2011).
- [29] M. Konoto, H. Imamura, T. Taniguchi, K. Yakushiji, H. Kubota, A. Fukushima, K. Ando, and S. Yuasa, *Appl. Phys. Express* **6**, 073002 (2013).
- [30] T. Taniguchi, H. Arai, H. Kubota, and H. Imamura, *IEEE Trans. Magn.* **50**, 1400404 (2014).
- [31] W. F. Brown Jr, *Phys. Rev.* **130**, 1677 (1963).